



This is a repository copy of *WC-CP: a Bluetooth low energy indoor positioning method based on the weighted centroid of the convex polygon.*

White Rose Research Online URL for this paper:

<https://eprints.whiterose.ac.uk/217998/>

Version: Published Version

---

**Article:**

Yan, J., Zhang, M., Yang, J. et al. (3 more authors) (2024) WC-CP: a Bluetooth low energy indoor positioning method based on the weighted centroid of the convex polygon. ISPRS International Journal of Geo-Information, 13 (10). 354. ISSN 2220-9964

<https://doi.org/10.3390/ijgi13100354>

---

**Reuse**

This article is distributed under the terms of the Creative Commons Attribution (CC BY) licence. This licence allows you to distribute, remix, tweak, and build upon the work, even commercially, as long as you credit the authors for the original work. More information and the full terms of the licence here:

<https://creativecommons.org/licenses/>

**Takedown**

If you consider content in White Rose Research Online to be in breach of UK law, please notify us by emailing [eprints@whiterose.ac.uk](mailto:eprints@whiterose.ac.uk) including the URL of the record and the reason for the withdrawal request.



[eprints@whiterose.ac.uk](mailto:eprints@whiterose.ac.uk)  
<https://eprints.whiterose.ac.uk/>

Article

# WC-CP: A Bluetooth Low Energy Indoor Positioning Method Based on the Weighted Centroid of the Convex Polygon

Jinjin Yan <sup>1,\*</sup>, Manyu Zhang <sup>1</sup>, Jinqun Yang <sup>1</sup>, Lyudmila Mihaylova <sup>2</sup>, Weijie Yuan <sup>3</sup> and You Li <sup>4</sup>

- <sup>1</sup> Qingdao Innovation and Development Center, Harbin Engineering University, Qingdao 266400, China; manyu.zhang@hrbeu.edu.cn (M.Z.); yjq980314@hrbeu.edu.cn (J.Y.)  
<sup>2</sup> Department of Automatic Control and Systems Engineering, The University of Sheffield, Sheffield S1 3JD, UK; l.s.mihaylova@sheffield.ac.uk  
<sup>3</sup> Department of Electrical and Electronic Engineering, Southern University of Science and Technology, Shenzhen 518055, China; yuanwj@sustech.edu.cn  
<sup>4</sup> State Key Laboratory of Surveying, Mapping and Remote Sensing, Wuhan University, Wuhan 430072, China; liyou@whu.edu.cn  
\* Correspondence: jinjin.yan@hrbeu.edu.cn; Tel.: +86-15321155969

**Abstract:** Indoor navigation has attracted significant attention from both academic and industrial perspectives. Indoor positioning is a critical component of indoor navigation. Several solutions or technologies have been proposed, such as Wi-Fi, UWB, and Bluetooth. Among them, Bluetooth Low Energy (BLE) is cost-effective, easily deployable, flexible, and efficient. This paper focuses on indoor positioning solely based on BLE. Motivated by two observations, namely, that (i) involving more anchor nodes can enhance positioning accuracy, and that (ii) narrowing the area for unknown location determination can also lead to improved accuracy, a new distance-based method, the Weighted Centroid of the Convex Polygon (WC-CP), is proposed. While it is generally acknowledged that incorporating more anchor nodes can enhance indoor positioning performance, the current state of the art lacks a robust methodology for selecting and utilizing these nodes. The WC-CP approach addresses this gap by introducing a systematic and efficient method for identifying and employing the most suitable anchor nodes. By avoiding nodes that could potentially introduce significant errors or lead to incorrect localization, our method ensures more accurate and reliable indoor positioning. The efficacy of WC-CP is demonstrated in an indoor environment, achieving an RMSE of 1.35 m. This result shows significant improvements over three state-of-the-art approaches, about 34.15% better than LSBM, 32.50% better than TWCBM, and 30.05% better than ITWCBM. These findings underscore the potential of WC-CP for enhanced accuracy and reliability in indoor positioning based on BLE.

**Keywords:** BLE; indoor positioning; RSSI; weighted centroid



**Citation:** Yan, J.; Zhang, M.; Yang, J.; Mihaylova, L.; Yuan, W.; Li, Y. WC-CP: A Bluetooth Low Energy Indoor Positioning Method Based on the Weighted Centroid of the Convex Polygon. *ISPRS Int. J. Geo-Inf.* **2024**, *13*, 354. <https://doi.org/10.3390/ijgi13100354>

Academic Editors: Ivana Ivánová, Yongze Song, Sisi Zlatanova and Wolfgang Kainz

Received: 10 July 2024

Revised: 30 September 2024

Accepted: 3 October 2024

Published: 6 October 2024



**Copyright:** © 2024 by the authors. Published by MDPI on behalf of the International Society for Photogrammetry and Remote Sensing. Licensee MDPI, Basel, Switzerland. This article is an open access article distributed under the terms and conditions of the Creative Commons Attribution (CC BY) license (<https://creativecommons.org/licenses/by/4.0/>).

## 1. Introduction

In recent decades, Location-Based Services (LBSs) have played a crucial role in transportation [1], medical services [2], and disaster management [3]. As the name implies, location or positioning is the core of LBS [4]. While Global Navigation Satellite Systems (GNSSs) have been widely used for outdoor positioning due to their all-weather capability, global coverage, and high accuracy, they are not suitable for indoor scenarios because of challenges such as occlusion and multi-path interference. Therefore, researchers and developers have focused on indoor LBS, especially developing various indoor positioning technologies/solutions, such as Infrared [5], Ultrasonic [6,7], Ultra-wide band (UWB) [8,9], RFID [10,11], ZigBee [12,13], WiFi [14], and Bluetooth Low Energy (BLE) [15,16].

BLE is a radio technology that supports short-distance communication for terminal devices. With the release of BLE 5.0, BLE devices have made significant improvements in terms of low-power consumption, high-speed connectivity, and effective transmission distance. Compared to other indoor positioning technologies, BLE has many advantages,

such as being low-cost, easily deployable, flexible, low power-consuming, highly compatible, stable, and secure [17]. Moreover, almost all mobile devices are equipped with BLE modules, which provide the hardware basis for BLE-based indoor positioning. In short, BLE is an economical, efficient, and user-friendly solution, particularly beneficial in environments with strict demands on budget, maintenance, and user privacy. Considering these factors, BLE emerges as a highly promising solution for indoor positioning. This research considers a purely BLE-based indoor navigation solution, because integrating BLE with other indoor positioning techniques, such as WiFi, has the potential to enhance functionality and accuracy, but such things often bring in other challenges. For example, because the Wi-Fi was originally not designed for indoor positioning, the integration may compromise positioning accuracy and pose threats to user privacy.

The positioning computation based on BLE can be categorized into two types: distance-based and non-distance methods. The former type mainly relies on the Received Signal Strength Indication (RSSI) [18]. In particular, after converting RSSI to distance, there are three commonly used methods for positioning computation, including signal time of arrival (TOA) [19], angle of arrival (AOA) [20,21], and time difference of arrival (TDOA) [22–24]. Researchers have conducted extensive investigations into distance-based methods for indoor localization. One notable example is the application of extreme value theory to improve the trilateration method [25]. In this approach, a non-linear error function is constructed by using the distances and positions of the anchor nodes. By finding the values that minimize this error function, the positions of the unknown nodes are further determined accurately. Other than that, a seminal work by [26] undertakes a comprehensive analysis by enumerating and categorizing potential error scenarios in trilateration techniques. To address these errors effectively, the authors propose separate estimation algorithms tailored to handle each specific error scenario. Building upon this foundational work, a novel geometric approach is introduced in [27], efficiently encompassing all the identified error scenarios mentioned in [26]. This method eliminates the need for laborious case-by-case handling, streamlining the localization process while improving overall accuracy. Additionally, a notable improvement to trilateration localization algorithms is presented in [28]. The proposed method calculates the uncertainty of ranging from all anchor nodes and strategically selects those with minimal uncertainty propagation by leveraging a sliding window optimization scheme. Accurate location estimates are then obtained using a least-squares criterion. This approach demonstrates commendable scalability, as it applies not only to trilateration measurements but also extends its utility to least-squares and maximum likelihood methods, resulting in high localization accuracy and acceptable efficiency.

The non-distance method uses RSSI directly rather than converting it into distance, as seen in the centroid-based method [29,30], Approximate Point In Triangulation Test (APIT) [31], and distance vector-hop (DV-Hop) [32]. The centroid-based method estimates a target's location by calculating the weighted average of multiple anchor node positions based on their RSSI values. Here, the RSSI from anchor nodes infers the relative proximity of the target to each anchor, allowing for an estimated location computation. APIT simplifies triangulation by approximating the target's position within a polygon formed by anchor nodes. It uses RSSI to determine whether the target lies inside or outside specific triangular regions, enabling efficient location estimation without requiring precise distance measurements. DV-Hop combines hop counts with estimated distances to infer the position of a target. Anchor nodes broadcast their positions along with the number of hops to the target, allowing it to estimate its location based on anchor positions and hop counts. This method is useful in scenarios where direct distance measurements may be unreliable, leveraging relative signal strengths for approximate location determination. However, non-distance methods generally have lower accuracy than distance-based methods, which rely on more precise calculations [25,33]. Therefore, this paper focuses on the distance-based method.

Among the distance-based methods, there are many efforts collectively to advance trilateration-based indoor localization by providing solutions to tackle errors, enhance precision, and achieve reliable position estimates across diverse scenarios. An improved

weighted centroid positioning method is presented in [34], which enhances accuracy by accounting for the weight of each beacon in scenarios with fewer anchors. Similarly, an indoor positioning algorithm based on polarization and the average RSSI-Weighted Three Minimum Distances (WTM) method is presented in [33]. This study conducts a comprehensive analysis of factors affecting positioning performance, establishes error rules, and verifies the relationship between distance and error, contributing to improved positioning accuracy. Additionally, a new Weighted Concentric Circle Generation (WCCG) method is proposed to address challenges in trilateration when no intersections or multiple intersections occur [35]. This approach employs the mean shift clustering method to effectively determine the locations of unknown nodes. However, such trilateration-based methods and their variants typically rely on only three anchor nodes for computing unknown locations. Theoretically, utilizing more anchor nodes can yield stronger signals and significantly enhance positioning accuracy [36]. This leads to the conclusion that incorporating a larger number of anchor nodes and minimizing the area designated for determining the unknown location can improve accuracy.

Motivated by two observations, that (i) involving more anchor nodes enhances positioning accuracy, and that (ii) narrowing the area for unknown location determination improves accuracy, a new distance-based method is proposed: the Weighted Centroid of the Convex Polygon (WC-CP). The remaining sections are organized as follows. Section 2 reviews three commonly used RSSI-based geometric methods, including the least squares-based method, the trilateration-based method, and its two variants. Section 3 presents WC-CP. Section 4 demonstrates the presented method with a case study, upon which conclusions and future work are drawn in the final section.

## 2. Related Work

BLE-based indoor positioning leverages signals emitted by BLE devices, and currently, two typical methods are employed to utilize these signals: the fingerprint-based method [37] and the geometric-based method [25]. The fingerprint-based approach involves matching received signals with pre-recorded fingerprints, making it cumbersome and complex, particularly when dealing with large databases of fingerprints. The process of data collection and updating can become unwieldy [38]. In contrast, the geometric-based method is known for its ease of implementation and requires less effort. Consequently, this study focuses on the geometric-based methods, specifically introducing three commonly used approaches: the least squares-based method [39,40], the trilateration-based method [41], and its two variants [25].

### 2.1. Least Squares-Based Method (LSBM)

The least squares-based method (LSBM) [39,40] is a positioning technique grounded in the least squares principle. This method calculates the distances between an unknown node and at least three non-collinear anchor nodes. It establishes a system of distance equations based on these measurements. Subsequently, it minimizes the sum of squared errors to derive the optimal estimated coordinates of the unknown node.

Figure 1 illustrates the principle of LSBM. Suppose there are  $n$  anchor nodes deployed in an indoor scene, in which their locations are  $(x_i, y_i) (i = 1, 2, \dots, n)$ . Then, the Euclidean distances between them and the unknown location are  $d_i (i = 1, 2, \dots, n)$  (Equation (1)).

$$\begin{cases} (x_1 - x)^2 + (y_1 - y)^2 = d_1^2 \\ (x_2 - x)^2 + (y_2 - y)^2 = d_2^2 \\ \vdots \\ (x_n - x)^2 + (y_n - y)^2 = d_n^2 \end{cases} \quad (1)$$

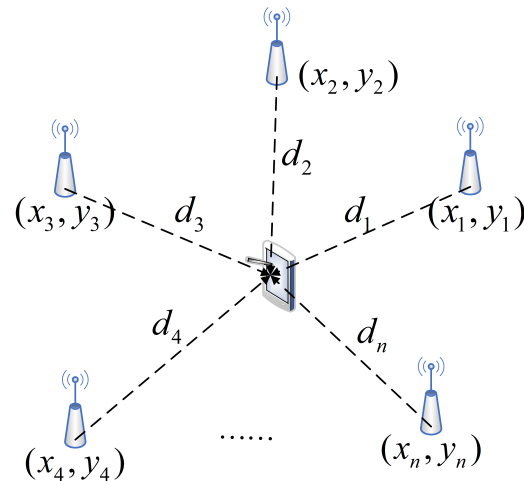


Figure 1. An illustration of LSBM.

Then, the above equation can be further processed as Equation (2), which could fit the form of  $AX = b$ , in which  $A$  and  $b$  are Equation (3). According to the principle of least squares, the location of unknown node  $(x, y)$  is  $X = (A^T A)^{-1} A^T b$ .

$$\begin{cases} x_1^2 - x_n^2 + y_1^2 - y_n^2 + d_n^2 - d_1^2 = 2(x_1 - x_n)x + 2(y_1 - y_n)y \\ x_2^2 - x_n^2 + y_2^2 - y_n^2 + d_n^2 - d_2^2 = 2(x_2 - x_n)x + 2(y_2 - y_n)y \\ \vdots \\ x_{n-1}^2 - x_n^2 + y_{n-1}^2 - y_n^2 + d_n^2 - d_{n-1}^2 = 2(x_{n-1} - x_n)x + 2(y_{n-1} - y_n)y \end{cases} \quad (2)$$

$$A = \begin{bmatrix} 2(x_1 - x_n) & 2(y_1 - y_n) \\ \vdots & \vdots \\ 2(x_{n-1} - x_n) & 2(y_{n-1} - y_n) \end{bmatrix} \quad b = \begin{bmatrix} x_1^2 - x_n^2 + y_1^2 - y_n^2 + d_n^2 - d_1^2 \\ \vdots \\ x_{n-1}^2 - x_n^2 + y_{n-1}^2 - y_n^2 + d_n^2 - d_{n-1}^2 \end{bmatrix} \quad (3)$$

## 2.2. Trilateration-Based Method (TBM)

The trilateration-based method (TBM) [41,42] determines the location of an unknown node by measuring the distances to three non-collinear anchor nodes. This method calculates coordinates of the unknown node by intersecting spheres (in three dimensions) or circles (in two dimensions) centered at the anchor nodes, with radii corresponding to the measured distances. TBM is commonly employed in GNSS navigation systems and other location-based applications.

As shown in Figure 2, assume that  $A(x_1, y_2)$ ,  $B(x_2, y_2)$ , and  $C(x_3, y_3)$  are three anchor nodes, and  $D(x, y)$  is the unknown node. The distances from  $D$  to the three anchor nodes are  $d_1$ ,  $d_2$ , and  $d_3$ , respectively (Equation (4)). Then, the location of  $D$  can be calculated based on Equation (5).

$$\begin{cases} (x_1 - x)^2 + (y_1 - y)^2 = d_1^2 \\ (x_2 - x)^2 + (y_2 - y)^2 = d_2^2 \\ (x_3 - x)^2 + (y_3 - y)^2 = d_3^2 \end{cases} \quad (4)$$

$$\begin{bmatrix} x \\ y \end{bmatrix} = \begin{bmatrix} 2x_1 - 2x_3 & 2y_1 - 2y_3 \\ 2x_2 - 2x_3 & 2y_2 - 2y_3 \end{bmatrix}^{-1} \times \begin{bmatrix} x_1^2 - x_3^2 + y_1^2 - y_3^2 + d_3^2 - d_1^2 \\ x_2^2 - x_3^2 + y_2^2 - y_3^2 + d_3^2 - d_2^2 \end{bmatrix} \quad (5)$$

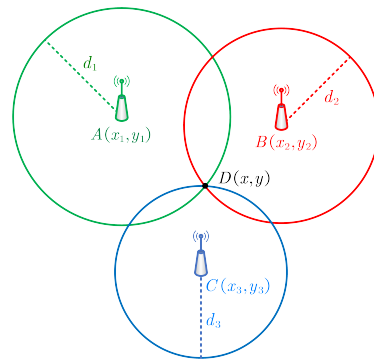


**Figure 2.** An illustration of TBM.

### 2.3. Variant I: Trilateral Weighted Centroid-Based Method (TWCBM)

Due to the random fluctuations of RSSI and the presence of various disturbance factors, the three circles in TBM may not intersect at a single point, rendering the method invalid (Figure 3). To address this issue, an upgraded version called the Trilateral Weighted Centroid-Based Method (TWCBM) [43] was proposed. TWCBM calculates the intersection points of the three circles and then determines the weighted centroid of the resulting triangle to estimate the position of the unknown node. For example, if the anchor nodes are  $A(x_a, y_b)$ ,  $B(x_b, y_b)$ , and  $C(x_c, y_c)$ , they can be connected as a triangle  $\triangle ABC$ . Then, the weighted centroid of the triangle is  $D(x, y)$ , which is regarded as the estimated position of the unknown location (Figure 3).

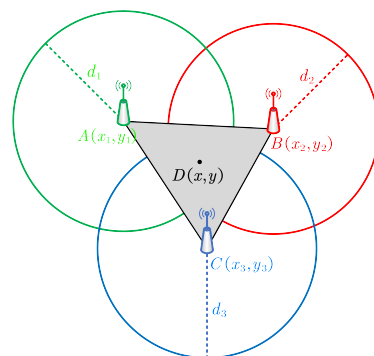


**Figure 3.** An illustration of TWCBM.

Generally, the closer an anchor node is to the unknown node, the less its RSSI is influenced by noise. This implies that a smaller transmission radius corresponds to a higher reliability of RSSI, and vice versa. The core idea of TWCBM is to utilize weights based on the distances between the unknown node and the anchor nodes, capitalizing on this relationship. A commonly used method for determining weights is to employ the reciprocal of the distance (Equation (6)). This approach ensures that the determination of the unknown node's location relies more heavily on less noisy RSSI, thereby enhancing its accuracy.

$$\begin{cases} x = \frac{x_1 \left( \frac{1}{d_2} + \frac{1}{d_3} \right) + x_2 \left( \frac{1}{d_1} + \frac{1}{d_3} \right) + x_3 \left( \frac{1}{d_2} + \frac{1}{d_1} \right)}{2 \left( \frac{1}{d_1} + \frac{1}{d_2} + \frac{1}{d_3} \right)} \\ y = \frac{y_1 \left( \frac{1}{d_2} + \frac{1}{d_3} \right) + y_2 \left( \frac{1}{d_1} + \frac{1}{d_3} \right) + y_3 \left( \frac{1}{d_2} + \frac{1}{d_1} \right)}{2 \left( \frac{1}{d_1} + \frac{1}{d_2} + \frac{1}{d_3} \right)} \end{cases} \quad (6)$$

### 2.4. Variant II: Improved Trilateral Weighted Centroid-Based Method (ITWCBM)

Building on the observation that narrowing the area for locating unknown nodes can enhance accuracy, an improved version of TWCBM, known as the Improved Trilateral

Weighted Centroid-Based Method (ITWCBM) [44], was proposed. In ITWCBM, the triangles used for centroid calculations are based on the intersection points of circles that represent the signal coverage of the anchor nodes, rather than the locations of anchor nodes themselves (Figure 4). Assuming that there are three anchor nodes  $A(x_1, y_1)$ ,  $B(x_2, y_2)$ , and  $C(x_3, y_3)$ , with distances to the unknown node being  $d_1$ ,  $d_2$ , and  $d_3$ , respectively, the coordinates of the intersection point  $a(x_a, y_a)$  can be calculated by using Equation (7).

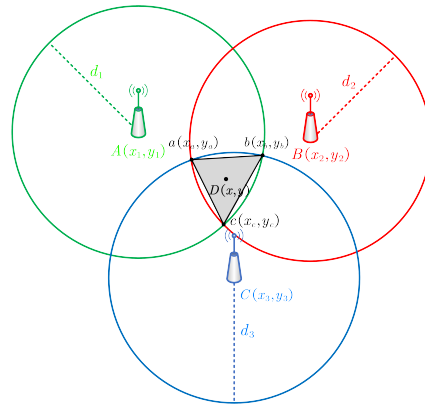


**Figure 4.** An illustration of ITWCBM.

$$\begin{cases} \sqrt{(x - x_a)^2 + (y - y_a)^2} \leq d_1 \\ \sqrt{(x - x_b)^2 + (y - y_b)^2} = d_2 \\ \sqrt{(x - x_c)^2 + (y - y_c)^2} = d_3 \end{cases} \quad (7)$$

Similarly, the coordinates of intersection points  $b$  and  $c$  are  $(x_b, y_b)$  and  $(x_c, y_c)$ , respectively. If the location of the unknown node is  $D(x, y)$ , its coordinates can be calculated by Equation (8):

$$\begin{cases} x = \frac{x_a \left( \frac{1}{d_1} + \frac{1}{d_2} \right) + x_b \left( \frac{1}{d_2} + \frac{1}{d_3} \right) + x_c \left( \frac{1}{d_3} + \frac{1}{d_1} \right)}{2 \left( \frac{1}{d_1} + \frac{1}{d_2} + \frac{1}{d_3} \right)} \\ y = \frac{y_a \left( \frac{1}{d_1} + \frac{1}{d_2} \right) + y_b \left( \frac{1}{d_2} + \frac{1}{d_3} \right) + y_c \left( \frac{1}{d_3} + \frac{1}{d_1} \right)}{2 \left( \frac{1}{d_1} + \frac{1}{d_2} + \frac{1}{d_3} \right)} \end{cases} \quad (8)$$

It is important to note that exceptional situations may arise, such as when the circles representing the signal areas of the anchor nodes do not intersect or contain each other (Figure 5). This can occur as the distance from the anchor nodes to the unknown node increases, leading to a higher probability of measurement error. In these cases, point  $C$  is considered to be positioned closer to anchor node  $B$ , thereby giving  $B$  greater influence in the calculation. The point  $C$  serves as an auxiliary reference for estimating the locations of unknown nodes, which is particularly beneficial when the anchor signal circles do not intersect or overlap. Suppose the radius of  $A(x_A, y_A)$  is  $d_1$ , and that of  $B(x_B, y_B)$  is  $d_2$ ; then, the position of  $C(x, y)$  can be calculated according to Equation (9).

$$\begin{cases} (y - y_A)(x_B - x_A) = (y_B - y_A)(x - x_A) \\ (x_A - x)^2 + (y_A - y)^2 = \left( \frac{d_1}{d_2} \right)^2 (x_B - x)^2 + (y_B - y)^2 \\ (x_A - x)^2 + (y_A - y)^2 + (x_B - x)^2 + (y_B - y)^2 = (x_B - x_A)^2 + (y_B - y_A)^2 \end{cases} \quad (9)$$

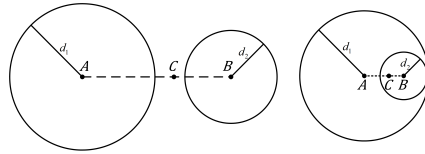


**Figure 5.** Two exceptional situations of ITWCBM.

### 2.5. Summary

Among the four commonly used methods, LSBM is the most straightforward. However, it may prove inadequate in certain situations. For instance, when anchor nodes are sparsely distributed, the matrix involved in LSBM can become ill-conditioned, resulting in unacceptable errors. Additionally, directly performing differential linearization can reduce accuracy, further compromising positioning stability. Compared to LSBM, TWCBM offers improved positioning accuracy to some extent. However, the search range for locating the unknown node remains large, potentially affecting the accuracy and reliability of the method. ITWCBM is an enhanced version of TWCBM that narrows the search range by using the intersection points of circles representing the signal areas of anchor nodes as the triangle vertices. Nevertheless, both TWCBM and ITWCBM randomly select three effective anchor nodes, which may not fully utilize all available anchor nodes. Therefore, it is argued that all four commonly used methods have limitations in localization accuracy.

### 3. The Weighted Centroid of the Convex Polygon Method (WC-CP)

The Weighted Centroid of the Convex Polygon (WC-CP) aims to enhance the positioning accuracy of unknown nodes by utilizing all effective anchor nodes and narrowing the area for location determination. This method involves selecting a set of anchor nodes that maintain effective communication with the unknown node, computing a convex polygon by connecting the intersection points of circles representing the signal areas of these anchor nodes, and calculating the weighted centroid of this convex polygon as the estimated location of the unknown node. Figure 6 illustrates WC-CP, featuring five anchor nodes ( $AN_1$  to  $AN_5$ ) and the colored polygon ( $P_{41}$ ,  $P_{42}$ ,  $P_{43}$ , and  $P_{44}$ ) as the area for determining the unknown location. WC-CP follows these five steps:

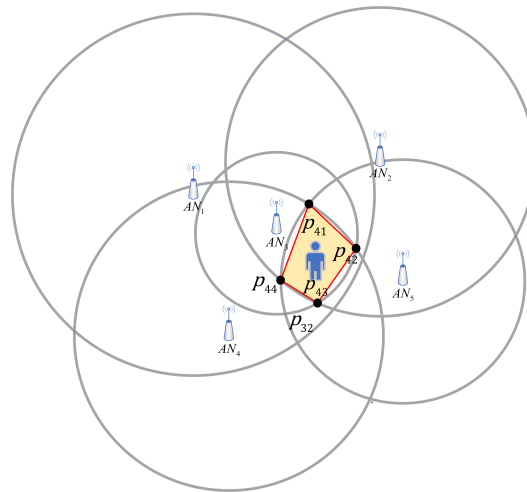


**Figure 6.** An illustration of WC-CP.  $AN_1$  to  $AN_5$  are five effective anchor nodes;  $P_{41}$ ,  $P_{42}$ ,  $P_{43}$ , and  $P_{44}$  are the vertices of the area for the unknown location determination.

- Step 1: Anchor node selection optimization. Identify the most effective anchor nodes for localization using a threshold segmentation method, which involves analyzing anchor node signals over time, setting thresholds, and segmenting the data accordingly.
- Step 2: Distance estimation. Estimate the distances between the unknown node and all anchor nodes based on RSSI.

- Step 3: The intersection points computation. Calculate all intersection points of circles representing the signal areas of valid anchor nodes in pairs.
- Step 4: Innermost convex polygon determination. Use the Graham scan algorithm [45] to iteratively eliminate the outermost convex polygon until the predetermined condition is met.
- Step 5: Position computation of unknown node. Compute the final position of the unknown node using a weighted method.

### 3.1. Anchor Node Selection Optimization

The RSSI of anchor nodes can be influenced by factors such as noise, interference, multipath fading, and environmental conditions, which complicate accurate distance estimation. To address these challenges, an effective selection method for choosing anchor nodes is essential. This can be based on criteria such as selecting the nodes with the strongest RSSI or those deemed most informative according to various metrics. This selection process aims to reduce the impact of noise and other error sources in the localization system, ultimately improving accuracy by utilizing the most reliable and informative anchor nodes.

In this paper, the selection method employs a fixed-length queue to manage the most recent RSSI values, thereby reducing the impact of outdated or irrelevant data. Specifically, consecutive raw RSSI values obtained from continuous sampling are processed in a sequence of fixed length ( $n$ ), i.e.,  $RSSI_{raw} = \{rssi_1, rssi_2, \dots, rssi_n\}$ . When a new RSSI arrives, the first element of the queue is popped out to maintain a stable queue length (Figure 7). After setting a threshold for RSSI ( $RSSI_{thre}$ ), the average of the moving RSSI ( $RSSI_{avg}$ ) is calculated based on Equation (10), and the RSSI is considered reference-able if it exceeds  $RSSI_{thre}$ . If  $RSSI_{avg}$  is less than or equal to  $RSSI_{thre}$ , the anchor node will be retained; otherwise, it will be removed because it will be judged as lack of reference ability. Finally,  $m$  anchor nodes that satisfy the threshold can be obtained, i.e.,  $rssi_1, rssi_2, \dots, rssi_m$ .

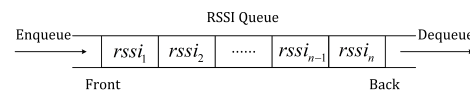


**Figure 7.** The recursive diagram of the RSSI queue.

$$RSSI_{avg} = \frac{1}{n} \sum_{i=1}^n RSSI_i \quad (10)$$

The queue length mentioned earlier is based on real-time data acquisition and processing, grounded in the theory of Age of Information (AoI) [46]. In this context, devices continuously collect RSSI data and maintain a fixed-length queue filled with the most recent samples. The advantage of AoI lies in its real-time capabilities, allowing the system to adapt swiftly to environmental changes or device movements. This flexibility makes the system applicable to diverse, complex indoor settings, and various use cases. When new RSSI data arrives, older information is dequeued to maintain a consistent queue size. This dynamic approach enables the system to promptly incorporate fresh signals, thereby enhancing the accuracy of distance position estimation between the device and reference nodes. As a result, both the precision and reliability of indoor localization are significantly improved.

The optimal  $RSSI_{thre}$  is determined using Bayesian analysis [47], which integrates prior knowledge with observed data to infer the probability distribution of unknown parameters. In this study, the process begins with an initial assumption for the RSSI threshold, represented as a prior probability distribution. This prior distribution is updated by continuously collecting actual RSSI data, resulting in a posterior probability distribution that provides a more accurate estimation of  $RSSI_{thre}$ . Through iterative Bayesian analysis, the estimation of  $RSSI_{thre}$  is gradually optimized, converging toward the most optimal value. This approach enhances our performance and accuracy in indoor positioning.

### 3.2. Distance Estimation

Several models can be employed to estimate the distances between an unknown node and anchor nodes. Two common models are the free-space propagation model [48] and the logarithmic distance loss model [49]. The free-space propagation model is primarily applicable in open spaces devoid of obstructions and multi-path effects. It considers only one factor, the energy attenuation per unit area caused by signal diffusion in space. However, wireless signals experience varying degrees of attenuation due to environmental factors. As the propagation distance increases and the path becomes more complex, the signal received by the mobile device is increasingly attenuated. In indoor environments, walls and other obstructions can cause significant occlusion and multi-path effects, making the free-space propagation model unsuitable. In contrast, the logarithmic distance loss model leverages the characteristic that the signal strength of a wireless signal decreases exponentially with increasing distance during propagation. This model is better suited for indoor environments where signal attenuation and multi-path effects are prevalent.

Therefore, this paper employs the logarithmic distance loss model (see Equation (11)).

$$RSSI_d = RSSI_{d_0} - 10\eta \lg\left(\frac{d}{d_0}\right) + \xi_\eta \quad (11)$$

where  $RSSI_d$  and  $RSSI_{d_0}$  are the RSSI when signals of BLE pass through a distance  $d$  and  $d_0$ , respectively, and  $\eta$  is the path loss index. In general,  $\eta$  will increase with the number of obstacles in the environment.  $\xi_\eta$  represents a zero-mean white Gaussian random variable with standard deviation  $\sigma$ .

In general,  $d_0$  is set as 1 m. According to Equation (11), the distance between an anchor node and the unknown node becomes Equation (12).

$$d = 10^{\left(\frac{RSSI_{d_0} + \xi_\eta - RSSI_d}{10\eta}\right)} \quad (12)$$

When the unknown node is within range of at least three anchor nodes, WC-CP can operate effectively. The parameter  $\eta$  in Equation (12) reflects the impact of the surrounding environment on ranging, making the selection of an appropriate  $\eta$  crucial. In the experimental setup, RSSI data are collected at varying distances with a fixed step length. The other two parameters are determined through fitting calculations, leading to the construction of a ranging mathematical model based on the experimental data. Finally, the set of distances from the effective anchor nodes to the unknown node is obtained by fitting the logarithmic distance loss model.

### 3.3. Computation of Intersection Points

After obtaining the set of  $m$  effective anchor nodes in the previous step, the next step is to compute the set of all intersection points between any two circles that represent the signal areas of the anchor nodes. Figure 8 illustrates the computing process of the intersection points between the circles of two anchor nodes,  $A(x_a, y_a)$  and  $B(x_b, y_b)$ , in which  $AB = d$ ,  $AE = a$ ,  $EB = b$ , and  $p_{ij}E = h$ . The set of intersection points can be denoted as  $P = \{p_{ij}(x_\kappa, y_\kappa)\}, i, j \in \{1, 2, \dots, m\}, \kappa = \{1, 2, \dots, \theta\}$ .

Then, the intersection points can be computed on the basis of Equation (13). If the circles that represent the signal regions do not intersect or overlap with each other, we have the exceptional situations of Section 2.4. Thus, the computations of the intersection points will follow Equation (9).

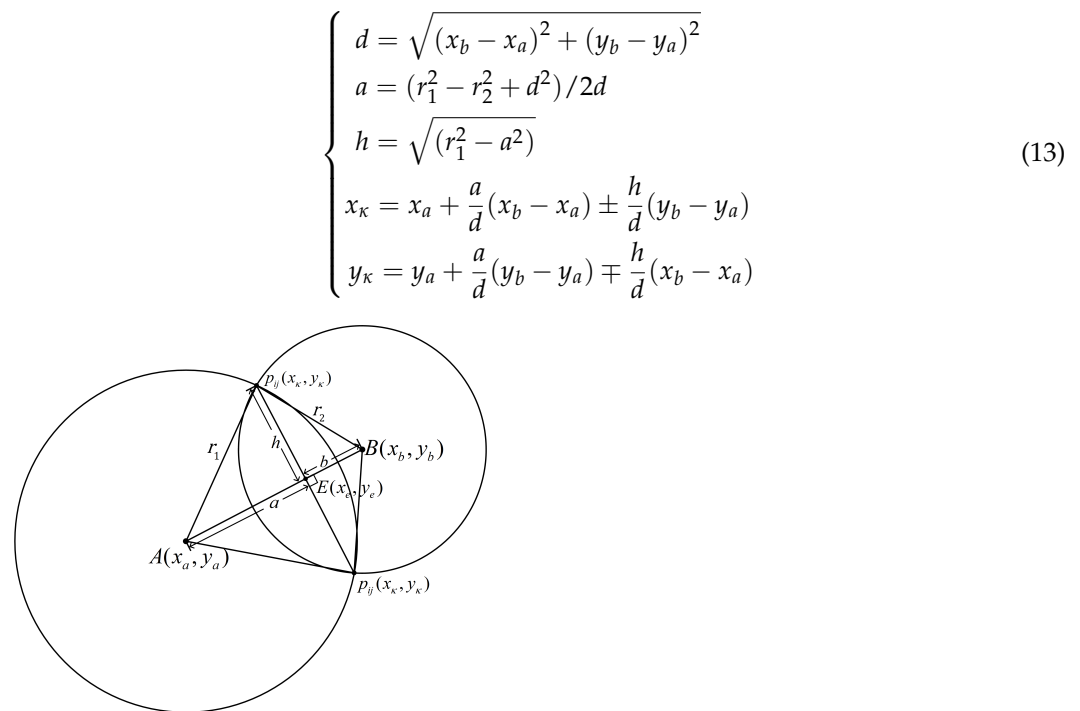


**Figure 8.** Illustration of intersection point computation between two circles.

### 3.4. Innermost Convex Polygon Determination

After obtaining the intersection points, the next step is to use the Graham scan algorithm [45] to find the innermost convex polygon, thereby achieving a final reduction of the localization area. The Graham scan algorithm is a widely used method for identifying the minimum convex polygon. It sorts the points by their polar angles with respect to a reference point and then constructs the convex polygon based on a scanning process.

Figure 9 illustrates the sequential process of calculating the convex hull using the Graham scan algorithm for a discrete point set consisting of five points. The output of the first iteration of the Graham scan algorithm is the minimum convex polygon (Figure 9d). The output of the first iteration of the Graham scan algorithm is the maximum convex polygon. The next step involves removing its vertices from the intersection set and check if the number of internal intersection points is less than or equal to the number of valid anchor nodes. If the above conditions are not met, the Graham scan algorithm may be used iteratively to find the maximum convex polygon until the innermost convex polygon satisfies the condition that the number of internal intersection points is less than or equal to the number of valid anchor nodes. The output of this process can be denoted as  $P = \{p_{ij}(x_\kappa, y_\kappa)\}, i, j \in \{1, 2, \dots, m\}, \kappa = \{1, 2, \dots, \varepsilon\}$ . The iterative elimination of the innermost convex polygon based on the Graham scan algorithm is detailed in Algorithm 1.

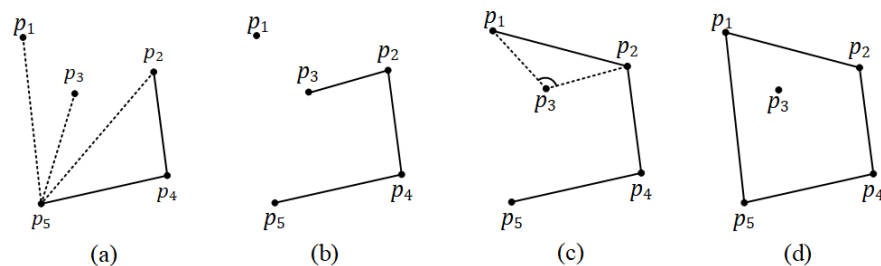


**Figure 9.** Illustration of Graham scan algorithm. (a) Sorting points by polar angle. (b) Constructing the initial convex hull. (c) Detecting concave angles and removing points. (d) Final convex hull constructed.

---

**Algorithm 1** The pseudo-code of eliminating the outermost convex polygon based on the Graham scan algorithm.

---

**Input:**  $P$ : Intersection points of all anchor nodes.  
**Output:**  $P$ : The points inside the convex hull.  
 $threshold \leftarrow$  The number of valid anchor nodes.  
**while** the length of  $P > threshold$  **do**  
     $p_0 \leftarrow$  point with lowest y-coordinate  
    **if** multiple points have the same y-coordinate **then**  
         $p_0 \leftarrow$  point with lowest x-coordinate  
    **end if**  
    Sort points in  $P$  by polar angle with respect to  $p_0$   
    Let  $S$  be an empty stack  
    **for**  $i \leftarrow 3$  to  $|P|$  **do**  
        **while**  $p_i$  turns right with respect to the top two points in  $S$  **do**  
            Pop the top point from  $S$   
        **end while**  
        Push  $p_i$  into  $S$   
    **end for**  
    Exclude the points in  $P$  that are in  $S$ .  
**end while**  
**return**  $P$

---

### 3.5. Position Computation of Unknown Node

After performing the aforementioned four steps, the position calculation process confines itself within the minimum convex polygon, which is based on the effective anchor node. Ultimately, the position of the unknown node is determined by computing the weighted centroid of the minimum convex polygon using Equation (14).

$$\begin{cases} x = \sum_{\kappa=1}^{\varepsilon} w_{\kappa} x_{\kappa} / \sum_{\kappa=1}^{\varepsilon} w_{\kappa} \\ y = \sum_{\kappa=1}^{\varepsilon} w_{\kappa} y_{\kappa} / \sum_{\kappa=1}^{\varepsilon} w_{\kappa} \end{cases} \quad \kappa = \{1, 2, \dots, \varepsilon\} \quad (14)$$

where  $(x_{\kappa}, y_{\kappa})$  represents the intersection coordinates of the anchor nodes, and  $w_{\kappa}$  represents the weight of the intersection points.

The weight coefficients are determined by taking the reciprocal sum of distances between nodes, and scaling coefficients are incorporated to mitigate the influence of longer distances and amplify the effect of shorter distances on localization results. Such coefficients serve as fine-tuning for the intersection points, which aims to balance the contributions of different distances to enhance the accuracy of localization. This method strengthens the association between anchor and unknown nodes and further improves the localization accuracy. The weight coefficient is defined by Equation (15)

$$\begin{cases} w_{\kappa(i,j)} = \left( \frac{1}{r_{\max}^{\varphi_1}} + \frac{1}{r_{\min}^{\varphi_2}} \right)^{\varphi_3} \\ r_{\max} = \max(r_i, r_j) \\ r_{\min} = \min(r_i, r_j) \end{cases} \quad i, j \in \{1, 2, \dots, m\} \quad (15)$$

where  $r_{\max}$  and  $r_{\min}$  represent the radii of the circles associated with the intersection points, in which the former is associated with the circle farthest from the unknown node, while the latter is the nearest. The three exponents  $\varphi_1$ ,  $\varphi_2$ , and  $\varphi_3$  are adjustable parameters related to the distance factors. Specifically,  $\varphi_1$  and  $\varphi_2$  modulate the impacts of the farthest and shortest distances, respectively.  $\varphi_3$  provides overall control for the curve characteristics of the weight function. The configuration of parameters  $\varphi_1$ ,  $\varphi_2$ , and  $\varphi_3$  can be adjusted based on empirical data or optimization algorithms to achieve the best localization accuracy.

## 4. Implementation and Case Study

### 4.1. Experiment Settings

The experiments were conducted in an indoor laboratory with a length of 20 m, a width of 10 m, and a height of 3.5 m (Figure 10a). Tests of indoor positioning in such a static scenario are commonly accepted, because such a practice can isolate the variables and provide a controlled test bed, whereas, for instance, the movement of people and furniture in the vicinity could potentially influence the results. In order to achieve a balance between factors such as signal coverage, localization reliability, system complexity, and deployment costs, a beacon interval of 4 m was chosen as a suitable compromise. This decision was made after evaluating various metrics, including accuracy requirements, signal characteristics, and installation convenience. The chosen spacing ensures satisfactory localization performance while managing expenses and simplifying deployment. Based on these considerations, a local coordinate system was established and nine BLE beacons (produced by MINEW TECHNOLOGIES (<https://www.minew.com/product-category/lbs-products/bluetooth-beacon/>) (accessed on 5 October 2024)) were deployed as anchor nodes at the following positions: A(6,0.5), B(6,4.5), C(6,8.5), D(10,8.5), E(10,4.5), F(10,0.5), G(14,0.5), H(14,4.5), and I(14,8.5). They were placed on top of shelf brackets (about 2 m) to simulate the deployment in real scenes, as anchor nodes are usually attached to the ceiling. Twenty-four distinct locations were selected as unknown nodes, simulating scenarios where users change their positions. In this experiment, their real locations were used as ground truth (Figure 10b).

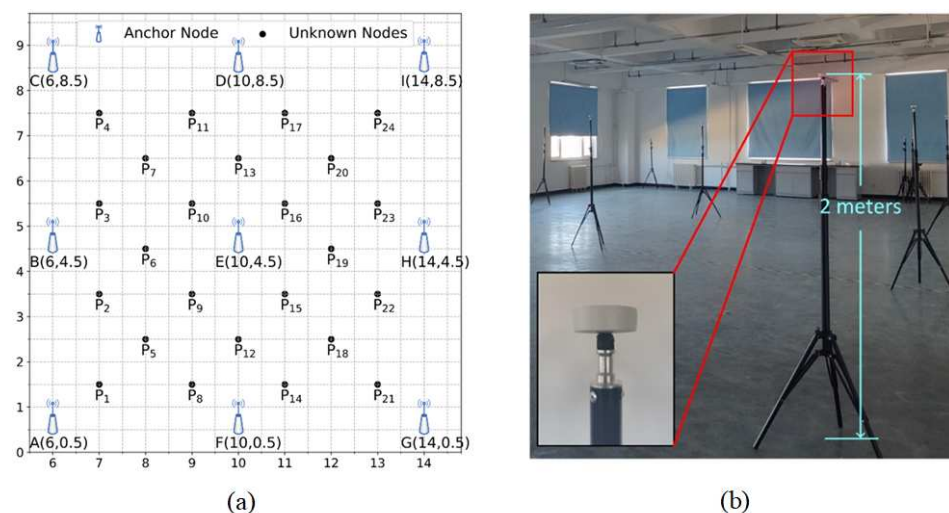


**Figure 10.** Experimental verification environment. (a) Layout of the experimental scenario, showing the positions of anchor nodes and unknown nodes (unit: m). (b) Example of a BLE beacon placed on top of shelf brackets.

To estimate the parameters for the logarithmic path loss equation (i.e.,  $RSSI_{d_0}$  and  $\eta$  in Equation (12)), a fixed anchor node was selected, and RSSI was measured using a cellphone at seven different distances, ranging from 1 to 7 m. At each measurement position, 200 RSSI samples were collected, and curve fitting was performed to determine the two parameters. The  $RSSI_{d_0}$  parameter was found to be  $-57.76$ , and  $\eta$  was 2.38. On the basis of iterative validation, the three weighting coefficients in Equation (15) were configured as  $\varphi_1 = 3$ ,  $\varphi_2 = 2.5$ , and  $\varphi_3 = 0.55$ .

Moreover, to compare the accuracy of different methods, two metrics, Root Mean Squared Error (RMSE) (Equation (16)) and Cumulative Distribution Function (CDF)

(Equation (17)), were employed. RMSE is used to evaluate the magnitude of positional error, while CDF can assess the error distribution. The expressions of the two metrics are:

$$RMSE = \sqrt{\frac{1}{n} \sum_{i=1}^n [(x - x')^2 + (y - y')^2]} \quad (16)$$

where  $(x, y)$  and  $(x', y')$ , respectively, represent the actual position coordinates of the unknown node and the position coordinates estimated by the localization service system.

$$F(x) = P(x \leq y) \quad (17)$$

where  $F(x)$  is the probability that the error value of the estimated position coordinate is below  $x$ , and  $y$  represents the allowable error value of positioning.

#### 4.2. Result Analysis

To evaluate the effectiveness of WC-CP, three other methods (LSBM, TWCBM, and ITWCBM) were also implemented. At each unknown location, 50 measurements were collected to minimize the effects of random errors. Figure 11 shows the estimated locations of the 24 unknown locations using WC-CP, along with their corresponding ground truth.

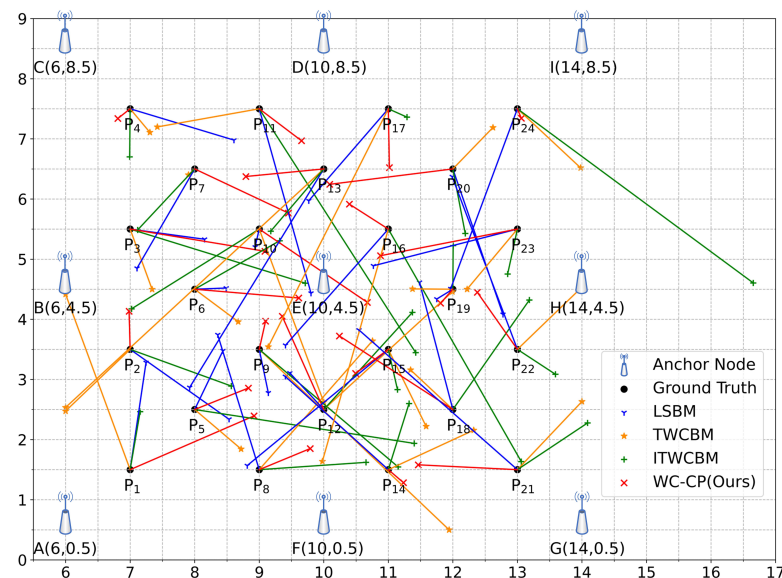


**Figure 11.** The results of different positioning methods (unit: m).

To better illustrate the positioning errors of WC-CP and the other three methods at each point, the average error of positioning of the 24 unknown nodes is plotted in Figure 12. The RMSE of the four methods is presented in Figure 13. The results indicate that WC-CP achieves an RMSE of 1.35 m, outperforming that of LSBM (2.05 m), TWCBM (2.0 m), and ITWCBM (1.93 m). This shows that the variance of WC-CP is significantly lower than that of the other three methods, and the positioning error distribution is more stable at each unknown node.

The CDF of the four methods (Figure 14) indicates that WC-CP outperforms the other three methods, achieving the highest localization accuracy at 1.9 m at 90% threshold, while the other three methods exceed 3 m. This indicates that the WC-CP method presented in this paper has significantly improved the positioning performance in terms of both accuracy and stability.

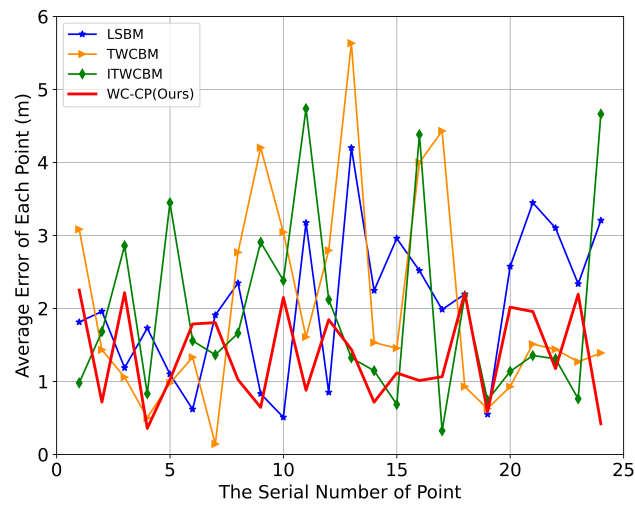


Figure 12. Point positioning error curves.

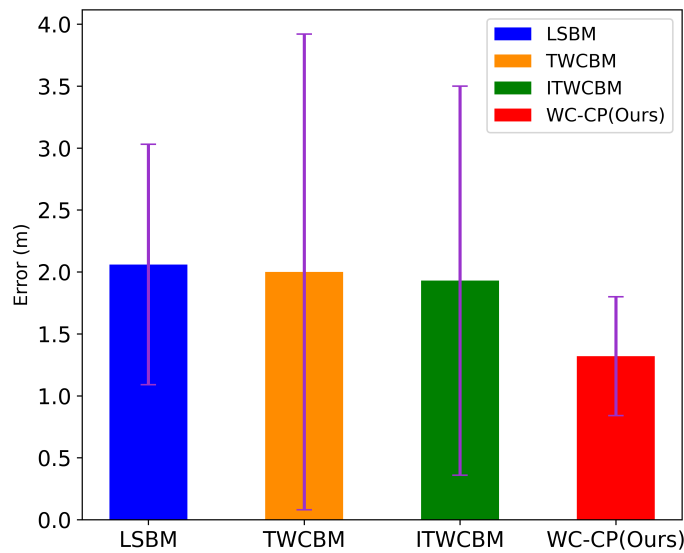


Figure 13. Errors of different positioning methods.

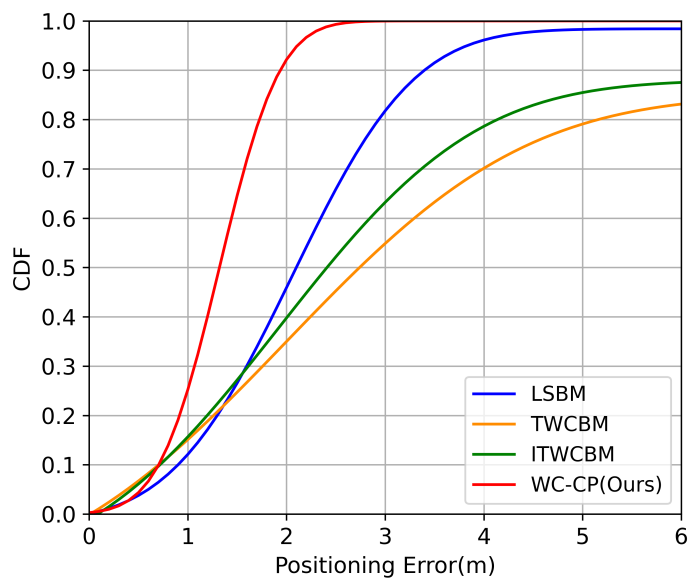


Figure 14. CDF of different positioning methods.

In summary, WC-CP outperforms the other three methods in positioning accuracy, particularly regarding stability. It demonstrates better performance in practical applications, suggesting its potential as a viable solution for enhancing the accuracy and overall performance of indoor positioning systems. Additionally, its resistance to environmental noise and ability to maintain good positioning accuracy make it a promising algorithm for future development and implementation.

#### 4.3. Discussion

The above experiments have demonstrated that WC-CP has advantages over other methods in terms of accuracy, stability, and resistance to environmental noise, but there are still some aspects that need to be addressed:

- **Distance estimation.** The logarithmic distance loss model is employed, as it can simulate the propagation of wireless signals relatively well. However, it requires continuous parameter adjustment and optimization to adapt to various experimental environments. There is also a certain degree of mismatch between the model and the actual environment, leading to sub-optimal ranging accuracy. Therefore, developing more accurate distance estimation models for indoor positioning systems remains essential.
- **Weight setting.** Another crucial aspect to consider in calculating the positions of unknown nodes is the weighting factor used. Typically, this factor is determined solely based on a distance-related parameter. However, the environment is in a constant state of flux, and relying solely on distance-related weighting factors can significantly impact localization results due to geographic disparities and the influence of the surrounding environment. As such, it is essential to adopt an appropriate method for adjusting weighting factors in a reasonable manner to reduce the error of localization results to some extent. Further research is required to develop more adaptive and dynamic algorithms that adjust weighting factors based on changes in the environment.
- **Anchor node deployment.** The geometric and topological relationships of anchor nodes significantly affect positioning performance and are thus a necessary condition for the reliable operation of the entire positioning service system. In this paper, anchor nodes are deployed in a regular fashion, i.e., evenly distributed over open space. However, such practice is overly idealistic and perhaps only appropriate for open experimental scenarios, and has limited flexibility, making it unsuitable for complex environments.
- **The potential impact of dynamic factors on positioning results.** The implementation and case study were conducted in a static indoor environment to isolate the variables and provide a controlled test bed for indoor positioning, which is a common approach to testing indoor positioning results. However, this does not take into account the potential impact of dynamic factors like people and furniture movement on the accuracy of the positioning. Therefore, future research will delve deeper into the potential impact of dynamic factors, such as the movement of people and furniture, on the accuracy and reliability of indoor positioning systems.
- **Expanding the WC-CP approach for practical applications, particularly in expansive indoor positioning systems, is indeed valuable.** One potential modification involves integrating adaptive algorithms that dynamically adjust parameters in response to real-time environmental changes. This enhancement would significantly improve the robustness of the system in complex settings.

#### 5. Conclusions and Future Work

This paper presents a novel indoor localization method named Weighted Centroid of the Convex Polygon (WC-CP). This method improves positioning accuracy and stability by involving more anchor nodes in the calculation and narrowing the area for unknown location determination. The experimental results show that WC-CP achieves an RMSE of 1.35 m, outperforming LSBM (2.05 m), TWCBM (2.0 m), and ITWCBM (1.93 m). Specifically,

WC-CP provides a 34.15% improvement over LSBM, a 32.50% improvement over TWCBM, and a 30.05% improvement over ITWCBM. Overall, these results show that WC-CP is a promising method for indoor positioning based on BLE, offering substantial gains in accuracy and reliability compared to existing approaches.

Future work will concentrate on further elaboration and testing of the current work as follows:

The limitations of existing distance models in accurately representing indoor environments have become apparent. As part of future research efforts, there will be a dedicated focus on the development of adaptive RSSI-based distance determination models, leveraging machine learning methodologies as a potential solution [50]. To mitigate the potential for significant positioning errors that can arise from using static weights in the calculation process of unknown node position, future research could explore the use of recursive updates of noise covariance and the dynamic adjustment of weights to optimize positioning and reduce the impact of anchor nodes on measurement nodes.

The deployment of anchor nodes is a challenging task due to the infinite solution space and multiple factors affecting the deployment. This problem is NP-hard [51], making it challenging to find an optimal solution. Heuristic algorithms such as swarm intelligence are widely used due to their faster solution speed and accuracy. Therefore, heuristic algorithms, artificial intelligence (AI), and machine learning (ML) will be employed to compute optimal strategies for the deployment of anchor nodes [52]. Such techniques could enhance the robustness and adaptability of the positioning system by allowing it to learn from various environmental conditions and historical data. Combining AI/ML algorithms with geometric methods is expected to achieve greater accuracy and reliability in complex indoor environments.

The experiments were conducted in an open indoor space without obstacles. In general, obstacles have substantially influenced signal propagation, reception, and reflection phenomena. Thus, the experimental configuration will be significantly enhanced to comprehensively account for the impact of obstacles. The plan involves incorporating prevalent obstructions typically found in real indoor settings to evaluate the performance and reliability of the proposed method. Moreover, the positions and properties of these obstacles will be meticulously measured and documented. This information will be shared with other researchers, promoting reproducibility and enhancing the experiment's overall dependability. Furthermore, more case studies will be conducted in more complex, real-world scenarios that closely mimic the dynamic nature of indoor environments, to improve the adaptability of the presented positioning algorithms that can better adapt to and compensate for these dynamic changes.

**Author Contributions:** Conceptualization, Jinjin Yan and Jinquan Yang; methodology, Manyu Zhang and Jinquan Yang; software, Jinquan Yang; validation, Jinjin Yan, Manyu Zhang, and Jinquan Yang; investigation, Jinjin Yan; resources, Lyudmila Mihaylova; writing—original draft preparation, Jinquan Yang; writing—review and editing, Manyu Zhang; visualization, Lyudmila Mihaylova; supervision, Weijie Yuan and You Li; project administration, Jinjin Yan; funding acquisition, Jinjin Yan. All authors have read and agreed to the published version of the manuscript.

**Funding:** This research was funded by the Shandong Province Natural Science Foundation Youth Branch (ZR2022QD121).

**Data Availability Statement:** The data that support the findings of this study are available from the corresponding author upon reasonable request.

**Conflicts of Interest:** The authors declare no conflicts of interest.

## References

1. Tan, Z.; Wang, C.; Yan, C.; Zhou, M.; Jiang, C. Protecting Privacy of Location-Based Services in Road Networks. *IEEE Trans. Intell. Transp. Syst.* **2021**, *22*, 6435–6448. [[CrossRef](#)]
2. Bibbò, L.; Carotenuto, R.; Della Corte, F. An Overview of Indoor Localization System for Human Activity Recognition (HAR) in Healthcare. *Sensors* **2022**, *22*, 8119. [[CrossRef](#)] [[PubMed](#)]

3. Fan, Z.; Cao, Y.; Zheng, B.; Wu, B.; Li, F. Geological Disaster Emergency Decision Support System based on Location-Based Service. In Proceedings of the 2022 International Conference on Computer Engineering and Artificial Intelligence (ICCEAI), Shijiazhuang, China, 22–24 July 2022; pp. 191–194.
4. Duong, N.S.; Dinh, T.M. Indoor Localization with Lightweight RSS Fingerprint Using BLE iBeacon on iOS Platform. In Proceedings of the 2019 19th International Symposium on Communications and Information Technologies (ISCIT), Ho Chi Minh City, Vietnam, 25–27 September 2019; IEEE: Piscataway, NJ, USA, 2019; pp. 91–95.
5. Ashhar, K.; Noor-A-Rahim, M.; Khyam, M.O.; Soh, C.B. A Narrowband Ultrasonic Ranging Method for Multiple Moving Sensor Nodes. *IEEE Sens. J.* **2019**, *19*, 6289–6297. [[CrossRef](#)]
6. Gabbrielli, A.; Bordoy, J.; Xiong, W.; Fischer, G.K.J.; Schaechtle, T.; Wendeberg, J.; Hoflinger, F.; Schindelbauer, C.; Rupitsch, S.J. RAILS: 3-D Real-Time Angle of Arrival Ultrasonic Indoor Localization System. *IEEE Trans. Instrum. Meas.* **2023**, *72*, 1–15. [[CrossRef](#)]
7. Wang, J.; Zhang, M.; Wang, Z.; Sun, S.; Ning, Y.; Yang, X.; Pang, W. An Ultra-Low Power, Small Size and High Precision Indoor Localization System Based on MEMS Ultrasonic Transducer Chips. *IEEE Trans. Ultrason. Ferroelectr. Freq. Control* **2022**, *69*, 1469–1477. [[CrossRef](#)]
8. Crețu-Sîrcu, A.L.; Schiøler, H.; Cederholm, J.P.; Sîrcu, I.; Schjørring, A.; Larrad, I.R.; Berardinelli, G.; Madsen, O. Evaluation and Comparison of Ultrasonic and UWB Technology for Indoor Localization in an Industrial Environment. *Sensors* **2022**, *22*, 2927. [[CrossRef](#)] [[PubMed](#)]
9. Yan, B.; Giorgetti, A.; Paolini, E. A Track-before-detect Algorithm for UWB Radar Sensor Networks. *Signal Process.* **2021**, *189*, 108257. [[CrossRef](#)]
10. Park, J.; Kim, Y.J.; Lee, B.K. Passive Radio-Frequency Identification Tag-Based Indoor Localization in Multi-Stacking Racks for Warehousing. *Appl. Sci.* **2020**, *10*, 3623. [[CrossRef](#)]
11. Perekadan, V.; Mukherjee, T.; Banerjee, C.; Pasilio, E. RF-MSiP: Radio Frequency Multi-source Indoor Positioning. In Proceedings of the 2019 IEEE International Conference on Big Data (Big Data), Los Angeles, CA, USA, 9–12 December 2019; pp. 5259–5268.
12. Latina, M.A.E.; Reyes, A.; Rollon, E.M. Optimization of RSSI-based Zigbee Indoor Localization System for Determining Distances Between Unknown Nodes. In Proceedings of the 2022 First International Conference on Electrical, Electronics, Information and Communication Technologies (ICEEICT), Trichy, India, 16–18 February 2022.
13. Fahama, H.S.; Ansari-Asl, K.; Kaviani, Y.S.; Soorki, M.N. An Experimental Comparison of RSSI-Based Indoor Localization Techniques Using ZigBee Technology. *IEEE Access* **2023**, *11*, 87985–87996. [[CrossRef](#)]
14. Liu, F.; Liu, J.; Yin, Y.; Wang, W.; Hu, D.; Chen, P.; Niu, Q. Survey on WiFi-based Indoor Positioning Techniques. *IET Commun.* **2020**, *14*, 1372–1383. [[CrossRef](#)]
15. Zhuang, Y.; Zhang, C.; Huai, J.; Li, Y.; Chen, L.; Chen, R. Bluetooth Localization Technology: Principles, Applications, and Future Trends. *IEEE Internet Things J.* **2022**, *9*, 23506–23524. [[CrossRef](#)]
16. Zafari, F.; Gkelias, A.; Leung, K.K. A Survey of Indoor Localization Systems and Technologies. *IEEE Commun. Surv. Tutor.* **2019**, *21*, 2568–2599. [[CrossRef](#)]
17. Shan, G.; Choi, G.; Roh, B.H. Bluetooth Low Energy-based Adaptive Scheme for IoT Services. In Proceedings of the 2023 Fourteenth International Conference on Ubiquitous and Future Networks (ICUFN), Paris, France, 4–7 July 2023; pp. 573–575. [[CrossRef](#)]
18. Kim Geok, T.; Zar Aung, K.; Sandar Aung, M.; Thu Soe, M.; Abdaziz, A.; Pao Liew, C.; Hossain, F.; Tso, C.P.; Yong, W.H. Review of Indoor Positioning: Radio Wave Technology. *Appl. Sci.* **2020**, *11*, 279. [[CrossRef](#)]
19. Krishnaveni, B.V.; Reddy, K.S.; Reddy, P.R. An Introduction to the TOA measurement for UWB indoor localization Systems. In Proceedings of the 2021 5th Conference on Information and Communication Technology (CICT), Kurnool, India, 10–12 December 2021; IEEE: Piscataway, NJ, USA, 2021; pp. 1–4.
20. Sollie, M.L.; Bryne, T.H.; Gryte, K.; Johansen, T.A. Reducing Ground Reflection Multipath Errors for Bluetooth Angle-of-Arrival Estimation by Combining Independent Antenna Arrays. *IEEE Antennas Wirel. Propag. Lett.* **2023**, *22*, 1391–1395. [[CrossRef](#)]
21. HajiAkhondi-Meybodi, Z.; Salimibeni, M.; Mohammadi, A.; Plataniotis, K.N. Bluetooth Low Energy and CNN-based Angle of Arrival Localization in Presence of Rayleigh Fading. In Proceedings of the ICASSP 2021—2021 IEEE International Conference on Acoustics, Speech and Signal Processing (ICASSP), Toronto, ON, Canada, 6–11 June 2021; IEEE: Piscataway, NJ, USA, 2021; pp. 7913–7917.
22. Deng, Z.; Zheng, X.; Zhang, C.; Wang, H.; Yin, L.; Liu, W. A TDOA and PDR Fusion Method for 5G Indoor Localization based on Virtual base Stations in Unknown Areas. *IEEE Access* **2020**, *8*, 225123–225133. [[CrossRef](#)]
23. Xiong, W.; Schindelbauer, C.; So, H.C.; Bordoy, J.; Gabbrielli, A.; Liang, J. TDOA-based localization with NLOS mitigation via robust model transformation and neurodynamic optimization. *Signal Process.* **2021**, *178*, 107774. [[CrossRef](#)]
24. Gültekin, B.; Kılıç, V.; et al. TDOA Based Indoor Localization of Wearable Smart Devices. In Proceedings of the 2021 29th Signal Processing and Communications Applications Conference (SIU), Istanbul, Turkey, 9–11 June 2021; IEEE: Piscataway, NJ, USA, 2021; pp. 1–4.
25. Yang, B.; Guo, L.; Guo, R.; Zhao, M.; Zhao, T. A Novel Trilateration Algorithm for RSSI-based Indoor Localization. *IEEE Sens. J.* **2020**, *20*, 8164–8172. [[CrossRef](#)]
26. Hwang, S.S.; Shin, S. Advanced TOA Trilateration Algorithm for Mobile Localization. In Proceedings of the 2018 IEEE 7th Asia-Pacific Conference on Antennas and Propagation, APCAP 2018, Auckland, New Zealand, 5–8 August 2018; pp. 543–544.

27. Hoang, M.L.; Rossi, J.P.; Slock, D. A Geometric Interpretation of Trilateration for RSS-based Localization. In Proceedings of the European Signal Processing Conference, Amsterdam, The Netherlands, 18–21 January 2021; pp. 1797–1801.
28. Yan, X.; Luo, Q.; Yang, Y.; Liu, S.; Li, H.; Hu, C. ITL-MEPOSA: Improved Trilateration Localization with Minimum Uncertainty Propagation and Optimized Selection of Anchor Nodes for Wireless Sensor Networks. *IEEE Access* **2019**, *7*, 53136–53146. [[CrossRef](#)]
29. Kaur, A.; Kumar, P.; Gupta, G.P. A weighted Centroid Localization Algorithm for Randomly Deployed Wireless Sensor Networks. *J. King Saud Univ.-Comput. Inf. Sci.* **2019**, *31*, 82–91. [[CrossRef](#)]
30. Rajasundari, T.; Balaji Ganesh, A.; HariPrakash, A.; Ramji, V.; Lakshmi Sangeetha, A. Weighted Trilateration and Centroid Combined Indoor Localization in Wifi Based Sensor Network. In Proceedings of the International Conference on Computer Networks, Big Data and IoT, Madurai, India, 19–20 December 2018; Springer: Cham, Switzerland, 2018; pp. 163–172.
31. Shen, X.; Xu, B.; Shen, H. Indoor Localization System Based on RSSI-APIT Algorithm. *Sensors* **2023**, *23*, 9620. [[CrossRef](#)] [[PubMed](#)]
32. Kanmaz, M.; Aydin, M. Comparison of dv-hop based indoor positioning methods in wireless sensor networks and new approach with k-means++ clustering method Kablosuz sensör ağlarda dv-hop tabanlı iç konumlandırma yöntemlerinin incelenmesi kiyaslanması ve K-means++ kümeleme yöntemi ile yeni yaklaşım. *J. Fac. Eng. Archit. Gazi Univ.* **2019**, *34*, 975–986.
33. Du, J.; Yuan, C.; Yue, M.; Ma, T. A Novel Localization Algorithm Based on RSSI and Multilateration for Indoor Environments. *Electronics* **2022**, *11*, 289. [[CrossRef](#)]
34. Zhang, X.; Zhang, S.; Huai, S. Low-Power Indoor Positioning Algorithm Based on iBeacon Network. *Complexity* **2021**, *2021*, 8475339. [[CrossRef](#)]
35. Ma, C.; Wu, B.; Poslad, S.; Selviah, D.R. Wi-Fi RTT Ranging Performance Characterization and Positioning System Design. *IEEE Trans. Mob. Comput.* **2022**, *21*, 740–756. [[CrossRef](#)]
36. Grinyak, V.; Devyatisilnyi, A.; Shurygin, A. Indoor 3D Positioning Based on Bluetooth Beacons. In *SMART Automatics and Energy: Proceedings of SMART-ICAE 2021, Vladivostok, Russia, 7–8 October 2021*; Springer Nature: Singapore, 2022; Volume 272; pp. 277–289.
37. Zhang, C.; Zhang, F.; Zhao, L. Research and optimization of BLE fingerprint indoor positioning algorithm based on fusion clustering. In Proceedings of the 2019 IEEE International Conference on Artificial Intelligence and Computer Applications (ICAICA), Dalian, China, 29–31 March 2019; IEEE: Piscataway, NJ, USA, 2019; pp. 95–100.
38. Ji, T.; Li, W.; Zhu, X.; Liu, M. Survey on indoor fingerprint localization for BLE. In Proceedings of the 2022 IEEE 6th Information Technology and Mechatronics Engineering Conference (ITOEC), Chongqing, China, 4–6 March 2022; IEEE: Piscataway, NJ, USA, 2022; Volume 6; pp. 129–134.
39. Valaee, S.; Champagne, B.; Kabal, P. Localization of wideband signals using least-squares and total least-squares approaches. *IEEE Trans. Signal Process.* **1999**, *47*, 1213–1222. [[CrossRef](#)]
40. Yan, B.; Zhu, B.; Chen, H.; Yang, Y.; Yang, J. Comparison of Indoor localization Methods in Two-Dimensional Wireless Sensor Network. In Proceedings of the 2020 International Conference on Communications, Information System and Computer Engineering (CISCE), Kuala Lumpur, Malaysia, 3–5 July 2020; pp. 18–29.
41. Chen, R.; Pei, L.; Liu, J.; Leppäkoski, H. WLAN and bluetooth positioning in smart phones. In *Ubiquitous Positioning and Mobile Location-Based Services in Smart Phones*; IGI Global: Hershey, PA, USA, 2012; pp. 44–68.
42. Pomárico-Franquiz, J.; Khan, S.H.; Shmaliy, Y.S. Combined extended FIR/Kalman filtering for indoor robot localization via triangulation. *Measurement* **2014**, *50*, 236–243. [[CrossRef](#)]
43. Zhao, J.; Zhao, Q.; Li, Z.; Liu, Y. An improved Weighted Centroid Localization algorithm based on difference of estimated distances for Wireless Sensor Networks. *Telecommun. Syst.* **2013**, *53*, 25–31. [[CrossRef](#)]
44. Mouhammad, C.S.; Allam, A.; Abdel-Raouf, M.; Shenouda, E.; Elsabrouty, M. BLE indoor localization based on improved RSSI and trilateration. In Proceedings of the 2019 7th International Japan-Africa Conference on Electronics, Communications, and Computations, (JAC-ECC), Alexandria, Egypt, 15–16 December 2019; IEEE: Piscataway, NJ, USA, 2019; pp. 17–21.
45. Zhang, B.; Xu, Y.; Wang, L.; Bi, S. Corner Point Recognition and Point Cloud Correction Based on Graham-Scan Algorithm. In Proceedings of the 11th International Conference on Computer Engineering and Networks, Hechi, China, 21–25 October 2021; Volume 808 LNEE, pp. 284–292.
46. Sun, Y.; Kadota, I.; Talak, R.; Modiano, E. Age of Information: A New Metric for Information Freshness. *Synth. Lect. Commun. Netw.* **2020**, *12*, 1–24.
47. Lindley, D.V. An Introduction to Bayesian Inference and Decision. *J. Oper. Res. Soc.* **1974**, *25*, 336–337. [[CrossRef](#)]
48. Onykienko, Y.; Popovych, P.; Yaroshenko, R.; Mitsukova, A.; Beldyagina, A.; Makarenko, Y. Using RSSI Data for LoRa Network Path Loss Modeling. In Proceedings of the 2022 IEEE 41st International Conference on Electronics and Nanotechnology (ELNANO), Kyiv, Ukraine, 10–14 October 2022; pp. 576–580.
49. El Khaled, Z.; Ajib, W.; McHeick, H. Log Distance Path Loss Model: Application and Improvement for Sub 5 GHz Rural Fixed Wireless Networks. *IEEE Access* **2022**, *10*, 52020–52029. [[CrossRef](#)]
50. Zi-xuan, D.; Jing, H.; Tie-cheng, S.; Lu, X. RSSI Indoor Ranging Method Based on Bluetooth Combining Hybrid Filtering and Neural Network. *Meas. Control Technol.* **2020**, *39*, 70–76.

51. Yuan, Z.; Li, W.; Yang, S. Beacon node placement for minimal localization error. In Proceedings of the 2019 International Conference on Internet of Things (iThings) and IEEE Green Computing and Communications (GreenCom) and IEEE Cyber, Physical and Social Computing (CPSCom) and IEEE Smart Data (SmartData), Atlanta, GA, USA, 14–17 July 2019; IEEE: Piscataway, NJ, USA, 2019; pp. 980–985.
52. Tilwari, V.; Pack, S.; Maduranga, M.; Lakmal, H. An Improved Wi-Fi RSSI-based Indoor Localization Approach Using Deep Randomized Neural Network. *IEEE Trans. Veh. Technol.* **2024**, 1–13. [[CrossRef](#)]

**Disclaimer/Publisher’s Note:** The statements, opinions and data contained in all publications are solely those of the individual author(s) and contributor(s) and not of MDPI and/or the editor(s). MDPI and/or the editor(s) disclaim responsibility for any injury to people or property resulting from any ideas, methods, instructions or products referred to in the content.